Balloon-borne Limb profiling of UV/vis skylight radiances, O3, NO2 and BrO: technical set-up and validation of the method

F. Weidner, H. Bösch, H. Bovensmann, J. P. Burrows, A. Butz, C. Camy-Peyret, M. Dorf, K. Gerilowski, W. Gurlit, U. Platt, et al.

Atmos. Chem. Phys. Discuss., 4, 7631–7665, 2004
www.atmos-chem-phys.org/acpd/4/7631/
SRef-ID: 1680-7375/acpd/2004-4-7631
European Geosciences Union

Atmospheric Chemistry and Physics Discussions

Balloon-borne Limb profiling of UV/vis skylight radiances, O_3, NO_2 and BrO: technical set-up and validation of the method

F. Weidner[1], H. Bösch[1,*], H. Bovensmann[3], J. P. Burrows[3], A. Butz[1], C. Camy-Peyret[2], M. Dorf[1], K. Gerilowski[3], W. Gurlit[3], U. Platt[1], C. von Friedeburg[1], T. Wagner[1], and K. Pfeilsticker[1]

[1]Institut für Umweltphysik, University of Heidelberg, Heidelberg, Germany
[2]Laboratoire de Physique Moléculaire et Applications (LPMA), Université Pierre et Marie Curie, Paris, France
[3]Institut für Umweltphysik und Fernerkundung, University of Bremen, Bremen, Germany
[*]now at: Jet Propulsion Laboratory (JPL), Pasadena, USA

Received: 9 August 2004 – Accepted: 28 October 2004 – Published: 24 November 2004

Correspondence to: K. Pfeilsticker (klaus.pfeilsticker@iup.uni-heidelberg.de)

Abstract

A novel light-weight, elevation scanning and absolutely calibrated UV/vis spectrometer and its application to balloon-borne Limb radiance and trace gas measurements is described. Its performance and the novel method of balloon-borne UV/vis Limb trace gas measurements has been tested against simultaneous observations of the same atmospheric parameters available from either (a) in-situ instrumentation (cf., by an electrochemical cell (ECC) ozone sonde also deployed aboard the gondola) or (b) trace gas profiles from inferred UV/vis/near IR solar occultation measurements performed on the same payload. The novel technique is also cross validated with radiative transfer modelling. Reasonable agreement is found (a) between measured and simulated Limb radiances and (b) inferred Limb O_3, NO_2 and BrO and otherwise measured profiles when properly accounting for all relevant atmospheric parameters (temperature T, pressure P, aerosol extinction, and major absorbers).

1. Introduction

In the past two decades remote sensing of the atmosphere by optical methods has evolved into a powerful tool for meteorological, atmospheric photochemistry and climate studies. Most recently, space-borne UV/vis Limb observations of the sky-light have also become available, cf. through the SOLSE/LORE, Odin/OSIRIS, Envisat/SCIAMACHY, METOP-IASI, ... instruments (e.g., Kerr et al., 1977; McElroy et al., 1988; Burrows et al., 1995; McPeters, et al., 2000; Von Savigny et al., 2003; Sioris et al., 2003).

The SCIAMACHY (SCanning Imaging Absorption spectroMeter for Atmospheric CHartographY) on the ESA-Envisat satellite offers unprecedented possibilities for atmospheric remote sensing by monitoring a larger number of atmospheric trace constituents by spectrally resolved UV/vis/near IR Limb observations. SCIAMACHY is a national contribution by Germany, the Netherlands and Belgium to the ESA-Envisat

satellite, which was launched into a sun synchronous low orbit on 28 February 2002 (Bovensmann et al., 1999). SCIAMACHY simultaneously measures the scattered or reflected atmospheric skylight in a variety of viewing directions and the extraterrestrial irradiance in the wavelength range from 220 nm to 2380 nm, at moderate spectral resolution (e.g., Rozanov et al., 2001; Eichmann et al., 2003; Kaiser and Burrows, 2003; Von Savigny et al., 2004a, b).

The UV/vis Limb measurements of SCIAMACHY, however, involve a number of novel methods and techniques which require careful validation and verification through collocated ground-based, aircraft, and balloon-borne measurements. Among them, the modelling and the verification of the atmospheric radiative transfer (RT) – including the investigation of its sensitivities to a larger number of atmospheric parameters (cf., the temperature, pressure ozone and aerosol profile, ...) – is most challenging for the interpretation of UV/vis Limb measurements (e.g., McElroy, 1988).

Following the pioneering studies of Kerr et al. (1977) and McElroy (1988), we report here on one of the most stringent tests ever to validate the individual steps (spectral retrieval, RT modelling and profile inversion) – and thus of the whole method – involved in the UV/vis Limb technique. For the present study we have chosen a twofold approach.

(1) The validation is performed by deploying a novel balloon-borne, and absolutely calibrated UV/vis scanning Limb spectrometer (called mini-DOAS) on a couple of stratospheric balloon flights on the azimuth controlled LPMA/DOAS payload (Laboratoire de Physique Moléculaire et Applications and Differential Optical Absorption Spectroscopy). These measurements allow us (a) to absolutely monitor UV/vis skylight radiances as a function of height, viewing geometry and solar zenith angle (SZA) and (b) by applying the Differential Optical Absorption Spectroscopy (DOAS, Platt, 1994; Platt and Stutz, 2004) technique to infer vertical profiles for a number of UV/vis absorbing atmospheric trace gases (O_3, NO_2, O_4, H_2O, BrO, and possibly in future of OClO, IO, OIO, ...).

(2) Further, the measured mini-DOAS Limb radiances are inter-compared to simulations of a novel Monte-Carlo (MC) radiative transfer model, the latter being used in

future studies for forward modelling of the SCIAMACHY Limb observations. Secondly, the inferred trace gas profiles from the mini-DOAS instruments are validated against simultaneous profile measurements of the same atmospheric constituents measured by well established in-situ (e.g., ozone by an electrochemical cell) or optical remote sensing techniques (cf., solar occultation) performed on the LPMA/DOAS payload. For details of the latter measurements see e.g., Camy-Peyret et al., 1993; Payan et al., 1998; Ferlemann et al., 2000; Harder et al., 1998, 2000; Bösch et al., 2003, and the companying paper of Gurlit et al., 2004).

The present study is organized as follows: In Sect. 2, the novel instrument and the radiative model used to interpret the measurement are briefly described. In Sect. 3, the instrument performance and its absolute calibration is described. In the Sects. 4 and 5, selected atmospheric observations of the mini-DOAS instrument are described and discussed with respect to the measurements of the other instruments also deployed aboard the LPMA/DOAS payload. Section 6 concludes the study with the lessons learned for future investigations.

2. Methods

2.1. Technical set-up of the mini-DOAS instrument

The novel mini-DOAS spectrometer has been designed for low weight (<4 kg) and low power consumption (7.5 W), with a particular emphasis being put on a stable imaging and a reasonably large signal to noise ratio. While the former characteristic offers the chance for versatile applications (cf., a stand-alone operation for time resolved measurements of important stratospheric radicals, trace gas measurements and radiative transfer studies in the cloudy troposphere), the latter feature is found to be necessary for the detection of O_3, NO_2 and in particular of the weakly absorbing gases (OClO, BrO, OIO, IO, ...), based on the experience with our larger precursor balloon spectrometer (Ferlemann et al., 1998, 2000; Harder et al., 1998, 2000; Bösch et al., 2003).

The mini-DOAS instrument consists of 5 major parts: (a) 2 light intake telescopes for simultaneous Nadir and scanning Limb observations (the latter being mounted on an automated elevation scanner), (b) glass fibre bundles which conduct the sky light from the telescopes into the spectrometers, (c) two commercial Ocean Optics USB-2000 spectrometers (d) which are mounted into an evacuated and thermo-stated housing, and finally (e) a single board computer for data handling and storage.

(a) The Nadir and Limb telescopes each consist of a spherical quartz lense (12.7 mm diameter, 30 mm focal length) which focuses the incoming scattered skylight onto the round or the rectangular entrance of the glass fiber bundles. During the balloon flight, the Nadir telescope is mounted at the bottom of the outer frame of the LPMA/DOAS payload structure, which provides an unobscured view into Nadir direction. The Limb telescope is mounted on an elevation angle scanner (built by Hofmann Meßtechnik, Rauenberg, Germany) which supports Limb observations in a range of $+10^{\circ}$ to -20° elevation angle, with step sizes as small as 0.04°. During the balloon flight, the scanner is mounted on the right hand side (i.e., in a $+90^{\circ}$ azimuth angle relative to the Sun's azimuth direction) of the azimuth controlled LPMA/DOAS gondola.

(b) Each glass fibre bundle consists of 10 individual quartz glass fibers each (diameter 100 μm, length 2 m, numerical aperture = 0.22). Glass fibre bundles are used, since they not only allow for a more flexible arrangement of the instrument, but are also known for largely reducing the polarization sensitivity of grating spectrometers (Stutz and Platt, 1996, 1997). In fact, laboratory measurements show that by using glass fibre bundles the polarization sensitivity of an Ocean Optics USB 2000 spectrometer is small ($\leq$1%). For the Nadir observations, the individual glass fibres are arranged in round geometry at the light intake, a mounting which together with the telescope supports a round field of view (FOV) of 0.6°. For the Limb observations the glass fibres are arranged in a 'rectangular geometry' light intake set-up i.e., the individual glass fibre entrances are linearly aligned. This arrangement supports a FOV of 0.19° in the vertical and 1.34° in the horizontal direction. Likewise, the glass fibres are linearly aligned at both exits, and the outgoing light is skimmed by a 50 μm wide and 1000 μm high

spectrometer entrance slit.

(c) The heart of the mini-DOAS balloon instrument consists of two commercial Ocean Optics USB 2000 spectrometers for simultaneous Nadir and Limb observations. The USB 2000 is a miniature grating spectrometer working in cross Czerny-Turner geometry. Its advantage is the small size ($86\times63\times30\,mm^3$), the low weight (270 g) and the high photon detection sensitivity owing to an integrated linear CCD array detector (Sony ILX511). The light enters the spectrometer through an entrance slit ($50\,\mu m\times1000\,\mu m$) from which it is focussed by a collimator mirror onto a holographic grating with 1800 grooves/mm. A second mirror focusses the light onto the linear CCD array with 2048 pixels (each pixel is 14 μm wide and 200 μm high). Attached onto the CCD array detector is a cylinder lense which focuses the 1000 μm high entrance slit onto the 200 μm high detector. Also attached to the CCD array detector is the preamplifier and a control logic unit which handles the pre-amplification of the signals, A/D conversion to 12 bit data and communication.

The spectrometers cover a spectral range of 327–527 nm at a full width at half maximum resolution (FWHM) of 0.8–1.0 nm, or 8 to 10 detector pixel/FWHM depending on the wavelength. Based on previous experience, this wavelength coverage and resolution should allow for the detection of the atmospheric trace gases O_3, NO_2, O_4, H_2O, BrO, and OClO (and potentially IO, OIO, CH_2O).

(d) Both spectrometers are kept in a sealed and evacuated container, which itself is immersed in a water-ice reservoir (~2 l). This ensures a stable spectrometer and CCD array temperature of 0°C during an entire balloon flight.

(e) Data handling and storage is maintained by a single board PC (type National Geode 200 MHz) which is equipped with a flash memory device. The allocated data are transferred from the spectrometers to the PC via a USB data transfer connection. It supports a data transmission rate fast enough to record a single spectrum every 25 ms. Possible integration times per spectrum as provided by the manufacturer of the spectrometers are in the range of 3–65 535 ms. The PC can alternatively be operated under Windows or the Linux operational systems with our lab-owned DOASIS or

XDOAS softwares packages, respectively. Both software tools support the automatic adjustment of the integration time, recording and storage of the measured spectra and the control of the Limb scanning stepper motor.

The total size of the instrument is 260×260×310 mm^3 (w/o fibers), its weight is ~4.8 kg plus 2 kg of water and ice, and its power consumption is ~7.5 W.

2.2. Radiative Transfer Modelling

A Monte Carlo (MC) Radiative Transfer model (called 'Tracy') has been developed by our group (Von Friedeburg, 2003). It allows the forward simulation of the mini-DOAS and Envisat/SCIAMACHY Limb observations. In particular, it can simulate the measured Limb radiances and slant column densities (SCD) of the trace gases under consideration, including sensitivity tests for varying atmospheric parameters such as T, P, the ozone and aerosol profiles.

'Tracy' solves the radiative transfer equation by backward Monte Carlo simulations in a full spherical, 3-dimensional and refractive atmosphere, based upon existing ray tracing routines. It does not, however, consider the polarization of the scattered skylight, which was found necessary in a recent theoretical study on scattered light ozone measurement (Hasekamp et al., 2002). Further, it supports an arbitrary spatial discretisation, a tool which permits to account for spatially strong varying aerosol and trace gas concentrations, and it takes into account multiple scattering with arbitrary scattering phase functions.

For the RT simulations, 'Tracy' uses atmospheric temperature and pressure profiles and if available profiles of the atmospheric aerosol and cloud cover and ozone profiles (Hönninger et al., 2004). For the present simulations, the stratospheric aerosol data version 2.00 of the SAGE III instrument is used (Thomason and Taha, 2003), and Mie scattering due to tropospheric clouds is not considered further. In the current version, 'Tracy' runs with either the 'Kurucz' (Kurucz et al., 1994) or the SOLSPEC solar spectrum (Thuillier et al., 1997, 1998a, b).

'Tracy' outputs are simulated wavelength dependent Limb radiances, slant column

densities (SCD) of the trace gases of interest which the actual measurements can be compared with, and so called box air mass factors (BoxAMFs). The latter are enhancement factors with respect to a vertical line of sight for the relative contribution of individual atmospheric layers on slant paths to the measured total absorption. Profile inversion from simulated or measured SCDs are performed by the optimal estimate a posteriori solution technique described in Rodgers (2000), also used for the inversion of solar occultation measurements performed by the other optical spectrometers (DOAS and LPMA) deployed on the gondola. The combined approach of forward modelling of the atmospheric RT, and 'conventional' profile inversion of simulated or measured SCDs is chosen since it offers the chance to cross validate each step of the novel developed 'quasi' in-situ Limb technique. Sensitivity tests and validation can thus be undertaken on the simulated and measured Limb radiance level, simulated or measured SCDs of the gases of interest, or by inter-comparison of inferred and otherwise measured profiles cf., obtained from the more traditional solar occultation technique. At the same time, the approach allows us to validate various radiative transfer codes used in upcoming studies addressing SCIAMACHY Limb observations.

3. Instrument performance and calibration

Instrument performance: The optical performance of the mini-DOAS instrument is tested in a set of laboratory measurements using alternatively Penray Hg, Kr or HgCd emission lamps or white lamp sources (PTFE integrating sphere BN-102-3 manufactured by Gigahertz or briefly Ulbricht sphere). For the temperature stabilized (to 0°C) instrument, the following relevant noise contributions (1σ rms) are found for single scans:

(a) an electron shot noise level of 15 binary units (BU) corresponding to a 1-σ noise of 0.474% for a 80% saturation level of the CCD array with a well-depth of 62 500 electrons and an electron to binary unit conversion factor of 15 e^-/BU.

(b) an electronic noise of 67.4 electrons or 4.4 BU causing a noise of 0.135% at 1-σ.

(c) the dark current of the SONY ILX511 shows a large pixel to pixel variation

e.g., next to pixels with very small dark current there are pixels for which the current is 270 electron/s corresponding to 18 BU/s. The average dark current, however, is 16.6 electrons/s only, corresponding to 1.09 BU/s, and the dark current noise is measured to 4.08 electrons/s, much smaller than the other noise contribution.

Since the noise contributions (a to c) suggest that the most significant noise sources are the photoelectron and offset noise, and both should be inversely proportional to the square root of the number of scans (N). The total noise is measured as a function of N (Fig. 1). For this purpose the total noise and its scaling with the number of scans is measured using scattered skylight and a small Ulbricht sphere. The latter is equipped with an up-to-date stabilized, quartz tungsten halogen (QTH) lamp. Test measurements alternatively using the lamp or skylight show that the 1-σ noise for single scans is 0.647% and 0.90% for the lamp and the skylight spectra, respectively. For a medium large number of scans, the instrument, in fact, operates at the physical limits given by the photo-electron noise. For an actual balloon flight, typically 100–1000 spectra (corresponding to 10–100 s integration time) are co-added for the sake of height resolution. This results for field conditions in a total 1-σ noise of $6{\cdot}10^{-4}$ for 100 (as indicated by the arrow in Fig. 1), and $2.5{\cdot}10^{-4}$ for 1000 co-added spectra, respectively (as indicated by the arrow in Fig. 1).

Absolute calibration: The radiometric calibration of both spectrometers is performed in two steps: In a first step, a small, but not absolutely calibrated, Ulbricht sphere is absolutely cross calibrated against an absolute radiance standard using the Limb spectrometer as transfer device. In a second step, this now absolutely calibrated integrating sphere is used for radiometric calibration of each of the spectrometers, shortly before the actual balloon flight is conducted.

For absolute radiance calibration, a NIST (National Institute of Standards and Technology) calibrated FEL 1000 W irradiance QTH standard (serial number F-455 from OSRAM Sylvania; Walker et al., 1987) in combination with a calibrated space grade Spectralon diffuser plate manufactured by Labsphere is employed. The same setup is used for absolute radiometric calibration of SCIAMACHY during the SCIAMACHY cal-

ACPD
4, 7631–7665, 2004

ibration campaign in 1998 (Dobber, 1999). The bi-directional reflectance distribution function (BRDF) of the diffuser plate is calibrated in 0–23° geometry by TNO/TPD. For more details see TNO/TPD report of calibration (van Leeuwen, 2003). NIST provides the calibration at a distance of 50 cm. The wavelength dependent radiometric irradiance accuracy of the NIST-FEL lamp ranges between 0.91%–1.09%, and the long term reproducibility is 0.87%–0.96% in the 350–654.6 nm wavelength range (for more details see the NIST report of calibration (844/25 70 96-96-1, 1997). For the radiance transfer measurements, the NIST-FEL lamp and the Spectralon diffuser plate are positioned into the optical axis given by the light intake of the Limb transfer spectrometer as recommended by Dobber (1999). The field of view of the spectrometer light intake telescope is small and completely located inside the characterized lamp irradiance plane on the Spectralon diffuser plate. After the measurement is taken, a not yet absolutely calibrated integrating sphere (type BN-102-3) is cross calibrated with the calibrated transfer spectrometer. The uncertainty of the radiance of the NIST-FEL lamp and Spectralon setup in the 300–700 nm region is 2–3% as indicated by test measurements performed during the SCIAMACHY calibration campaign (Gerilowski, 2004). For the somewhat less ideal conditions in the field, the estimated accuracy of the absolute radiometric calibration for both spectrometers is assessed to 35% at 380 nm, 10% at 440 nm and 4% at 510 nm, including all known sources of uncertainties and errors. The reproducibility of the integrating sphere measurements is better than 1%, respectively.

Further, the absolute calibration is checked by comparing the measured radiance at two wavelengths (360 nm vs. 490 nm), for a condition for which the radiative transfer is simple. For example, for the Limb observations (90° azimuth angle, +0.5° elevation angle, SZA=88.54° at 30 km) during the Kiruna 23 March 2003 flight, by far most photons (≥98%) are single Rayleigh scattered. Therefore, by knowing the relative solar irradiance F(360 nm)/F(490 nm)=0.588 (e.g. Gurlit et al., 2004) for the two wavelengths and the relative probability for Rayleigh scattering $(490\,\text{nm})/(360\,\text{nm})^4=3.432$, the radiance ratio I(360 nm)/I(490 nm)=2.018 can be calculated. In fact, the model 'Tracy' calculates a ratio of I(360 nm)/I(490 nm)=2.06, and our observation yields

I(360 nm)/I(490 nm)~2.0.

4. Observations and flights

For the actual balloon flights (see Table 1) the instrument is mounted on the azimuth controlled LPMA/DOAS payload. One of the telescopes is directed into the Nadir, whereas the other telescope is mounted into the Limb scanner, which points perpendicular to the Sun's azimuth direction (when the gondola is perfectly azimuth controlled).

To date 5 mini-DOAS flights have been performed; and overall the instrument performed well during all of them. Since the instrument and method are novel and need some testing, the instrument has been constantly refined by cf., by operating a Limb scanner from the second flight on, by subsequently improving the instrument's housing and cooling and its software, and finally by adding a vacuum sealed housing surrounding the spectrometers. Therefore, the Limb and Nadir spectra are not directly comparable from one balloon flight to another. Nevertheless, the functionality, and the feasibility of the method, as well as its potential for novel atmospheric observations are well demonstrated by the results discussed in the following section.

5. Results and discussion

In the following, we provide some sample results obtained from the data collected during 2 of the 5 balloon flights:

(a) In a first exercise, the measured absolute skylight radiances (azimuth angle 90°, fixed elevation of +0.5°) are compared with MC modelled skylight radiances for two wavelengths (λ=360 nm and λ=490 nm) for the balloon ascent and the balloon float altitude (30.3–32.2 km) Limb scanning observations at Kiruna on 23 March 2003 (Figs. 2 and 3). For the RT modelling the actual measured atmospheric parameters (profiles of T and p, and of ozone) are used, and the ground albedo is set to 0.6 (which accounts for the still existing snow cover over Northern Scandinavia by late March 2003).

ACPD
4, 7631–7665, 2004

No further assumptions are made for the tropospheric aerosols and cloud scattering and absorption, mainly because they are not known for the actual sounding and are known to be quite variable. Figure 2 demonstrates that with the given assumptions the measured stratospheric Limb radiances at 360 nm and 490 nm are reasonably reproduced well by the RT model (within the given error bars). At λ=360 nm, however, the measured Limb radiances are exceedingly larger than the simulation below 17 km, most likely due to the Mie scattering of very small aerosols (r<0.01 μm) not captured in the SAGE-III measurements and not accounted for in the RT simulations even though claimed to be a real feature (Hirsekorn, 2003). Also not unexpected, in the tropopause region the measured Limb radiances are much more variable at 490 nm than at 360 nm. This effect is due to the predominance of Mie scattering by aerosols and clouds over Rayleigh scattering for the skylight radiances in the visible (at 490 nm) compared to UV light (at 360 nm).

Figure 3 shows the measured and modelled Limb radiance λ=490 nm for the Limb scanning observations at balloon float altitude (30.3–32.2 km). Overall, a good agreement in the measured and modelled skylight radiance is found for Limb scanning runs (number 2 to 5 when counting from left to right), and only for the 1st run (around SZA=89°) the disagreement is larger at lower altitudes than expected. We believe that the gap around SZA=90° is due to the notorious difficulties of RT models to deal numerically correct with 1/cos(SZA)-issues in this regime. Test runs using a better numerical representation are under way. Moreover, sensitivity tests showed that increasing the ground or tropospheric albedo can partly (but not totally) close the gap between lower measured than modelled radiance received from the lowermost stratosphere.

(b) After gaining some confidence in the RT modelling and the involved numerical inversion techniques (for the latter see e.g., Rodgers, 2000; Ferlemann et al., 1998, 2000), we further evaluate the measured spectra during balloon ascent and at balloon float to obtain profile information of some relevant atmospheric absorbers in the UV/vis wavelength range i.e., of O_3, NO_2, O_4, BrO, and H_2O, and, in future studies of OClO.

For the evaluation of O_3, NO_2, O_4, BrO and H_2O slant column densities (SCD),

the Differential Optical Absorption Spectrometry (DOAS) technique is applied to the measured spectra (Platt, 1994; Platt and Stutz, 2004). For the spectral retrieval, the WinDOAS programme is used (M. Van Roozendael and C. Fayt, private communication). In the spectral retrieval of the different gases, the following wavelength intervals with following reference spectra are considered: 490–520 nm for O_3 and H_2O; 400–450 nm for NO_2 465–490 nm for O_4, and 347–358 nm for BrO, NO_2, O_4 and O_3. For trace gas reference absorption spectra, the following spectra are used: ozone from Burrows et al. (1999) (at T=203 K and 223 K) and alternatively from Voigt et al. (2001) (T=203 K); NO_2 (T=217 K) from Harder et al. (1997) (T=217 K and 230 K); O_4 (at room temperature) from Hermans et al. (personal communication, 2002; for details see also: http://www.oma.be/BIRA-IASB/Scientific/Topics/Lower/LaboBase/acvd/O4Info.html); for BrO (T=223 K) from Wahner et al. (1988) shifted by +0.25 nm to match the wavelength calibration of the BrO reference from the IUP-Bremen (see http://www.iup.physik.uni-bremen.de/gruppen/molspec/bro2_page.html); and water vapor (T=230 K, p=400 hPa) from Rothman et al. (2003). All high resolution cross sections are convolved with the actual instrumental slit function, determined from recorded line spectra of Hg and Kr. A spectrum correcting for the Ring effect is also included in the fitting routine (Grainger and Ring, 1962). For the Fraunhofer reference spectrum, a Limb measurement from balloon float altitude is used, for which the residual trace gas absorptions are expected to be minimal. For example, for the flight from Kiruna on 23 March 2003, the Fraunhofer reference is recorded at an altitude of 29 746 km, SZA=88.5°, elevation angle +0.5° and azimuth angle 90° to the sun. Figures 4 and 5 show the spectral retrievals for the inferred differential slant column densities of ozone measured at 31 620 km for SZA=89.9°, and elevation angle −5.5°, and of NO_2 measured at 30 940 km for SZA=89.4°, and −3.5° elevation angle, respectively. Figure 6 shows the inferred BrO absorption for an observation at 26 439 km altitude (−1.5° elevation angle, 90° azimuth angle and SZA=82.9°) for the Kiruna flight on 24 March 2004. The trace gas amounts in the Fraunhofer references are determined by a DOAS fit of the measured spectra to the Kurucz (Kurucz et al., 1984) spectrum convolved to

the instrument's resolution.

In a first exercise, we tested the O_3 profile retrieval from the mini-DOAS observations for a fixed Limb viewing geometry (at an azimuth angle of 90° and an elevation angle of 0.5°) performed during the balloon ascent of the Kiruna 23 March 2003 flight. Note that the balloon flight is undertaken around the vortex edge, implying large horizontal gradients in the trace gas concentrations.

In a first step, the slant column densities of ozone (O_3-SCD) are inferred from the measured spectra, and compared with the same parameter simulated by Tracy RT calculations using as input either the O_3 profile simultaneously measured aboard by an electrochemical cell (ECC), or by a stand-alone ECC O_3 sonde, launched ~3 h after the LPMA/DOAS gondola. Figure 7 reveals that the measured and simulated O_3-SCDs compare reasonably well, however only for the simulations using the ozone profile measured by the ECC-sonde aboard (the full line in Fig. 7). Conversely taking the O_3 profile in the simulation from the measured stand-alone launched ECC sonde launched ~3 h after the LPMA/DOAS payload, larger O_3 concentrations are obtained in the 12–21 km height range with a corresponding overestimation in the simulated O_3-SCDs (dotted curve in Fig. 7). This comparison clearly demonstrates the quality of the Limb O_3 measurements and its sensitivity towards the shape and O_3 concentration of the profile. This large sensitivity for upper tropospheric and lower stratospheric trace gas detection is also indicated by the averaging kernels which attain a value close to unity within the 4.5 km to 29 km height range (on a 1 km altitude grid below 20 km and 2 km above 20 km (see Fig. 8).

In a second step, the measured O_3-SCDs are mathematically inverted into O_3 profile, using RT simulated air mass factors for each observation, and the inversion routines described in Sect. 2.2 (Fig. 9). Overall, the good agreement found between the inferred Limb ozone profile and the simultaneously measured O_3 profiles either from the aboard ECC sonde or inferred from the direct Sun DOAS observations indicates the feasibility of the balloon-borne Limb method.

In a second exercise, we inferred from the measured NO_2-SCDs, a NO_2 profile for the balloon ascent on 23 March 2003 (Fig. 10). As before the comparison of the NO_2 profiles inferred either from the Limb or direct Sun observations is excellent. As before, this finding again demonstrates the equally large sensitivity of the balloon-borne ascent Limb measurement compared to the solar occultation techniques. It is a result of the trade of the larger sensitivity for the solar occultation vs Limb scanning spectroscopy due to the larger amount of analyzed photons, and the smaller averaging kernels (or air mass factors) for the former vs the latter measurements.

In a third exercise, we inferred from the measured Limb spectra the BrO profile for the balloon ascent on 24 March 2004 (Fig. 11). As for the NO_2 comparison, the Limb measured BrO excellently compares with the BrO measured with the solar occultation instrument, thus providing compelling confidence in both methods.

Finally in a fourth exercise, we inter compare measured and simulated O_3 Limb profiling for the Kiruna 23 March 2003 balloon float (30.3–32.2 km) observations (Fig. 12). As before, the measured and simulated O_3-SCDs compare well, in particular for tangent heights above the ozone maximum concentration (>25 km). For lower altitudes, simulated O_3-SCD are larger than those measured, a finding for which the reason is not totally clear. Noteworthy is however, that the simulated O_3-SCDs are less sensitive to RT errors than the simulated Limb radiances. Therefore the small error found in the simulated radiance (Fig. 3) can hardly provide an explanation for the discrepancies. Moreover, the RT simulations show that most photons (~95%) contributing to the measured spectrum are single scattered into the instrument's field of view. In consequence, for a given ozone profile, a larger simulated than measured Limb O_3-SCD could mean a longer simulated than real viewing distance (or a better visibility) over which the Limb radiance received by the instrument is integrated. Conversely, if the RT model simulations fit well with the actual atmospheric RT, smaller measured than simulated O_3-SCDs would imply smaller ozone concentrations than assumed in the simulation (here as before, the aboard measured ECC-sonde ozone profile is taken). In fact, there is a good reason to assume that the latter explanation is more likely than

the former since the measurement is performed at the vortex edge. Therefore the low-in-ozone polar vortex air masses are coming more and more into the instrument's field of view as the gondola followed (in clockwise direction) the increasing solar azimuth angle with progressing balloon flight duration.

6. Conclusions

We describe first measurements of a novel UV/vis spectrometer and its application to balloon-borne Limb radiance and trace gas measurements. The study discusses the instrument's performance in a series of balloon flights, and the novel method of balloon-borne UV/vis Limb trace gas measurements is tested against simultaneous observations of the same atmospheric parameters and RT model results.

Overall a reasonably good agreement is found in inter-comparisons of simulated and measured Limb radiance performed in fixed observing geometry during balloon ascent, and in Limb scanning geometry at balloon float altitude during sunset. Due to potential problems arising from the Earth sphericity and atmospheric refraction, the latter provides a stringent test for forward RT modelling. Further, accurate and cross validated RT modelling and measurements, however, permit to calculate more reliably photolysis frequencies of UV/vis absorbing atmospheric trace gases, known to be particularly difficult to be calculated at large solar zenith angles (e.g., Bösch et al., 2001; Uhl and Reddmann, 2004). The inter-comparison demonstrates that the UV/vis optical properties of the stratosphere for volcanically quiescent and polar stratospheric cloud free periods are reasonably well understood.

The novel quasi 'in-situ' Limb technique is also cross validated by simultaneous measurements of the same atmospheric trace gases (here O_3, NO_2, BrO) and, overall, a good agreement is found. It is shown that the UV/vis Limb measurements are particularly sensitive in the upper troposphere/lowermost stratosphere (UT/LS) for moderately large SZA during balloon ascent. In the future, this particularly large sensitivity may allow more accurate studies on the UT/LS NO_2 or halogen oxide photochemistry than

presently available from remote sensing instrumentation. Moreover, scanning UV/Vis Limb profiling may provide a rather powerful tool to investigate the time dependent photochemistry of stratospheric radicals, for example of the ClO+BrO ozone loss cycle by simultaneous observations of the OClO and BrO profiles in the wintertime polar stratosphere (WMO, 2002).

Finally, our study demonstrates the overall feasibility of the various methods (spectral retrieval, forward RT modelling, profile inversion, ...) in the emerging technique of satellite-borne remote sensing of atmospheric constituents by spectroscopic UV/vis Limb observations (e.g., Burrows et al., 1995; McPeters, et al., 2000; Von Savigny et al., 2003; Sioris et al., 2003).

Acknowledgements. Support of the project by BMBF through grants 50FE0017 and 50FE0019. We are grateful to the support given by the team of CNES in particular 'l'equipe nacelles pointées' and the balloon launching team from Aire-sur-l'Adour/France for the assistance given to perform successfully the balloon flights. We thank in particular C. Randall (University of Colorado, Boulder, USA) for providing the SAGE III aerosol data. Thanks to M. Long for English proof-reading the manuscript.

References

Bösch, H., Camy-Peyret, C., Chipperfield, M., Fitzenberger, R., Harder, H., Schiller, C., Schneider, M., Trautmann, T., and Pfeilsticker, K.: Inter comparison of measured and modeled stratospheric UV/vis actinic fluxes at large solar zenith angles, Geophys. Res. Lett., 28, 1179–1182, 2001.

Bösch, H., Camy-Peyret, C., Chipperfield, M. P., Fitzenberger, R., Harder, H., Platt, U., and Pfeilsticker, K.: Upper limits of stratospheric IO and OIO inferred from center-to-limb-darkening-corrected balloon-borne solar occultation visible spectra: Implications for total gaseous iodine and stratospheric ozone, J. Geophys. Res., 108, D15, 4455, doi:10.1029/2002JD003078, 2003.

Bovensmann, H., Burrows, J. P., Buchwitz, M., Frerick, J., Noöel, S., Rozanov, V. V., Chance, K. V., and Goede, A. H. P.: SCIAMACHY: Mission Objectives and Measurement Modes, J. Atmos. Sci., 56, 127–150, 1999.

Burkholder, J. B. and Talukdar, R. K.: Temperature dependence of the ozone absorption cross section over the wavelength range 410 to 760 nm, Geophys. Res. Lett., 21, 581–584, 1994.
Burrows, J. P., Hölzle, E., Goede, A. P. H., Visser, H., and Fricke, W.: SCIAMACHY – Scanning Imaging Absorption Spectrometer for Atmospheric Chartography, Acta Astronautica, 35, 7, 445, 1995.
Burrows, J. P., Richter, A., Dehn, A., Deters, B., Himmelmann, S., Voigt, S., and Orphal, J.: Atmospheric remote-sensing reference data from GOME – 2. Temperature-dependent absorption cross sections of O_3 in the 231–794 nm range, J. Q. S. R. T., 61, 4, 509–517, 1999.
Camy-Peyret, C., Flaud, J. M., Perrin, A., Rinsland, C. P., Goldman, A., and Murcray, F.: Stratospheric N_2O_5, CH_4 and N_2O profiles from IR solar occultation spectra, J. Atmos. Chem., 16, 31–40, 1993.
Dobber, M.: Absolute radiometric calibration of the SCIAMACHY PFM, TNSCIA1000TP/190, issue 1, Feb. 15, 1999.
Eichmann, K.-U., Kaiser, J. W., von Savigny, C., Rozanov, A., Rozanov, V., Bovensmann, H., König, M., and Burrows, J. P.: SCIAMACHY limb measurements in the UV/vis spectral region: first results, Adv. Space Res., 34, 775–779, 2003.
Ferlemann, F., Camy-Peyret, C., Fitzenberger, R., Harder, H., Hawat, T., Osterkamp, H., Perner, D., Platt, U., Schneider, M., Vradelis, P., and Pfeilsticker, K.: Stratospheric BrO Profiles Measured at Different Latitudes and Seasons: Instrument Description, Spectral and Profile Retrieval, Geophys. Res. Lett., 25, 3847–3850, 1998.
Ferlemann, F., Bauer, N., Fitzenberger, R., Harder, H., Osterkamp, H., Perner, D., Platt, U., Schneider, M., Vradelis, P., and Pfeilsticker, K.: A new DOAS-instrument for stratospheric balloon-borne trace gas studies, J. Appl. Opt., 39, 2377–2386, 2000.
Gerilowski, K.: Estimation of the Absolute Value of the ESM Diffuser BRDF from NASA Sphere Measurements from Optec-5, IFE-SCIA-KG-20040128_ESM_BRDF_Correction, draft 1.3, May 15, 2004.
Gil, M., Puentedura, O., Yela, M., and Cuevas, E.: Behaviour of NO_2 and O_3 columns during the eclipse of 26 February 1998, as measured by visible spectroscopy, J. Geophys. Res., 105, 3583–3593, 2000.
Grainger, J. F. and Ring, J.: Anomalous Fraunhofer line profiles, Nature, 193, 762, 1962.
Gurlit, W., Bösch, H., Butz, A., Burrows, J., Camy-Peyret, C., Dorf, M., Gerilowksi, K., Weidner, F., and Pfeilsticker, K.: Stratospheric solar irradiance in the UV-A, abd visible spec-

tral ranges: Inter-comparison with ground-based and satellite-borne measurements, Atmos. Chem. Phys. Discuss., accepted, 2004.
Harder, J. W., Brault, J. W., Johnston, P., and Mount, G. H.: Temperature dependent NO_2 cross sections at high spectral resolution, J. Geophys. Res., 102, 3861–3879, 1997.
Harder, H., Camy-Peyret, C., Ferlemann, F., Fitzenberger, R., Hawat, T., Osterkamp, H., Perner, D., Platt, U., Schneider, M., Vradelis, P., and Pfeilsticker, K.: Stratospheric BrO Profiles Measured at Different Latitudes and Seasons: Atmospheric Observations, Geophys. Res. Lett., 25, 3843–3846, 1998.
Harder, H., Bösch, H., Camy-Peyret, C., Chipperfield, M., Fitzenberger, R., Payan, S., Perner, D., Platt, U., Sinnhuber, B., and Pfeilsticker, K.: Comparison of measured and modeled stratospheric BrO: Implications for the total amount of stratospheric bromine, Geophys. Res. Lett., 27, 3695–3698, 2000.
Hasekamp, O. P., Landgraf, J., and van Oss, R.: The need of polarization modeling for ozone profile retrieval from backscattered sunlight, J. Geophys. Res., 107, 4692, doi:10.1029/2002JD002387, 2002.
Hirsekorn, M.: Measurements of Stratospheric Aerosol Extinction Coefficients by Balloon-borne DOAS Observations, Diploma thesis, University of Heidelberg, Heidelberg, Germany, 2003.
Hönninger, G., von Friedeburg, C., and Platt, U.: Multi Axis Differential Optical Absorption Sepctroscopy (MAX-DOAS), Atmos. Chem. Phys., 4, 231–254, 2004, SRef-ID: 1680-7324/acp/2004-4-231.
Kaiser, J. W. and Burrows, J. P.: Fast weighting functions for retrievals from Limb scattering measurements, J. Q. S. R. T., 77, 273–283, 2003.
Kerr, J. B., Evans, W. F. J., and McConnell, J. C.: The effect of NO_2 changes at twilight on tangent ray NO_2 measurements, Geophys. Res. Lett., 4, 577–579, 1977.
Kurucz, R. L., Furenhild, I., Brault, J., and Testermann, L.: Solar Flux Atlas From 296 to 1300 nm, National Solar Observatory Atlas, No. 1, June 1984.
McElroy, C. T.: Stratospheric nitrogen dioxide concentrations as determined from limb brightness measurements made on June 17th, 1983, J. Geophys. Res., 93, 7075–7083, 1988.
McPeters, R. D, Janz, S. J., Hilsenrath, E., Brown, T. L., Flittner, D. E., and Heath, D. F.: The retrieval of O_3 profiles from Limb scatter measurements: Results from the Shuttle Ozone Limb Sounding Experiment, Geophys. Res. Lett., 27, 2597–2600, 2000.
Payan, S., Camy-Peyret, C., Lefèvre, F., Jeseck, P., Hawat, T., and Durry, G.: First direct simultaneous HCl and $ClONO_2$ profile measurements in the Arctic vortex, Geophys. Res.

Lett., 25, 2663–2666, 1998.
Platt, U.: Differential Optical Absorption Spectroscopy (DOAS), Air Monit. by Spectr. Techniques, edited by: Sigrist, M. W., Chemical Analysis Series, 127, 27–84, John Wiley & Sons, Inc., 1994.
Platt, U. and Stutz, J.: Differential Optical Absorption Spectroscopy (DOAS), Principle and Applications, Springer Verlag Heidelberg, ISBN 3-340-21193-4, 2004.
Rodgers, C. D.: Inverse Methods For Atmospheric Sounding, World Scientific, Singapore, New Jersey, London, Hongkong, 2000.
Rothman, L. S., Barbe, A., Benner, D. C., Brown, L. R., Camy-Peyret, C., Carleer, M. R., Chance, K., Clerbaux, C., Dana, V., Devi, V. M., Fayt, A., Flaud, J.-M., Gamache, R. R., Goldman, A., Jacquemart, D., Jucks, K. W., Lafferty, W. J., Mandin, J.-Y., Massie, S. T., Nemtchinov, V., Newnham, D. A., Perrin, A., Rinsland, C. P., Schroeder, J., Smith, K. M., Smith, M. A. H., Tang, K., Toth, R. A., Vander Auwera, J., Varanasi, P., and Yoshino, K.: The HITRAN molecular spectroscopic database: edition of 2000 including updates through 2001, J. Q. S. R. T., 82, 1–4, 2003.
Rozanov, A., Rozanov, V., and Burrows, J. P.: A numerical radiative transfer model for a spherical planetary atmosphere: Combined differential-integral approach involving the Picard iterative approximation, J. Q. S. R. T., 69, 513–534, 2001.
Sioris, C. E., Haley, C. S., McLinden, C. A., von Savigny, C., McDade, I. C., McConnell, J. C., Evans, W. F. J., Lloyd, N. D., Llewellyn, E. J., Chance, K. V., Kurosu, T. P., Murtagh, D., Frisk, U., Pfeilsticker, K., Bösch, H., Weidner, F., Strong, K., Stegman, J., and Mégie, G.: Stratospheric profiles of nitrogen dioxide observed by OSIRIS on the Odin satellite, J. Geophys. Res., 108, 4215, doi:10.1029/2002JD002672, 2003.
Stutz, J. and Platt, U.: Numerical analysis and estimation of the statistical error of differential optical absorption spectroscopy measurements with least-square methods, Appl. Opt., 35, 30, 6041–6053, 1996.
Stutz, J. and Platt, U.: Improving long-path differential optical absorption spectroscopy (DOAS) with a quartz-fiber mode-mixer, Appl. Opt., 36, (6), 1105–1115, 1997.
Thomason, L. W. and Taha, G.: SAGE III aerosol extinction measurements: Initial Results, Geophys. Res. Lett., 30, (12), 1631, doi:10.1029/2003GL017317, 2003.
Thuillier, G., Hersé, M., Simon, P. C., Labs, D., Mandel, H., and Gillotay, D.: Observation of the UV solar irradiance between 200 and 350 nm during the ATLAS-1 mission by the SOLSPEC spectrometer, Sol. Phys., 171, 283–302, 1997.

Thuillier, G., Hersé, M., Simon, P. C., Labs, D., Mandel, H., Gillotay, D., and Foujols, T.: The visible solar spectral irradiance from 350 to 850 nm as measured by the SOLSPEC spectrometer during the ATLAS-1 mission, Sol. Phys., 177, 41–61, 1998a.

Thuillier, G., Hersé, M., Simon, P. C., Labs, D., Mandel, H., and Gillotay, D.: Solar radiometry and solar spectral irradiance: Observation of the solar spectral irradiance from 200 nm to 870 nm during the ATLAS 1 and ATLAS 2 missions by the SOLSPEC spectrometer, Metrologia, 35, 689–697, 1998b.

Uhl, R. and Reddmann, T.: Divergence of sun-rays by atmospheric refraction at large solar zenith angles, Atmos. Chem. Phys., 4, 1399–1405, 2004, SRef-ID: 1680-7324/acp/2004-4-1399.

Van Leeuwen, S.: Spectralon Diffuser BRDF Measurement, ESA Technical Note, TPD-SCIAPhE-TN-009, issue 1, Sept. 3, 2003, and Absolute Radiometric Calibration of the SCIAMACHY PFM, TNSCIA1000TP/190, issue 1, Feb. 15, 1999.

Von Friedeburg, C.: Derivation of Trace Gas Information combining Differential Optical Absorption Spectroscopy with Radiative Transfer Modelling, PhD Thesis, IUP Heidelberg, Heidelberg 2003.

Von Savigny, C., Rozanov, A., Bovensmann, H., Eichmann, K.-U., Kaiser, J. W., Noël, S., Rozanov, V. V., Sinnhuber, B.-M., Weber, M., and Burrows, J. P.: Stratospheric Ozone Profiles retrieved from Limb Scattered Sunlight Radiance Spectra Measured by the OSIRIS Instrument on the Odin Satellite, Geophys. Res. Lett., 30, doi:10.1029/2002GL016401, 2003.

Von Savigny, C., Rozanov, A., Bovensmann, H., Eichmann, K.-U., Kaiser, J. W., Noël, S., Rozanov, V. V., Sinnhuber, B.-M., Weber, M., and Burrows, J. P.: The Ozone hole break-up in September 2002 as seen by SCIAMACHY on Envisat, J. Atmos. Sci., in press, 2004a.

Von Savigny, C., Kokhanovsky, A., Bovensmann, H., Eichmann, K.-U., Kaiser, J., Noël, S., Rozanov, A. V., Skupin, J., and Burrows, J. P.: NLC Detection and Particle Size Determination: First Results from SCIAMACHY on Envisat, Adv. Space Res., in press, 2004b.

Voigt, S., Orphal, J., Bogumil, K., and Burrows, J. P.: The Temperature dependence (203–293 K) of the absorption cross sections of O_3 in the 230–850 nm region measured by Fourier-transform spectroscopy, J. Photochem. Photobiol. A, 143, 1–9, 2001.

Wahner, A., Ravishankara, A. R., Sander, S. P., and Friedl, R. R.: Absorption cross section of BrO between 312 and 385 nm at 298 and 223 K, Chem. Phys. Lett., 152, 507–512, 1988.

Walker, K. D., Saunders, R. D., Jackson, J. K., and Mc Sparron, D. A.: Spectral Irradiance Calibration, NBS Special Publication, 250–20, 1987.

World Meteorological Organization (WMO): Scientific Assessment of ozone depletion 2002: WMO Global Ozone Research and Monitoring Project, No. 47, chap. 7, Geneva, Switzerland, 2002.

Table 1. Compendium of balloon-borne mini-DOAS measurements and Envisat/SCIAMACHY overpasses

Date Time (UT)	Location	Geophys. Cond. SZA range	Instrument	Observation Mode	Closest Match Orbit# Time (UT) (i)
18/19 Aug. 2002 15:15–2:38	Kiruna 67.9° N, 21.1° E	high lat. sum. 69.75–94.4° 94.6–88.1°	LPMA/ mini-DOAS	Nadir fixed Limb	2429: 9:17, 9:19 2438: 9:48, 9:51
4 March 2003 12:55–15:25	Kiruna 67.9° N, 21.1° E	high lat. spring 77.6–88.8°	LPMA/DOAS mini-DOAS	Nadir fixed Limb	5272: 9:26, 9:28 5273: 11:04, 11:05, 11:07
23 March 2003 14:47–17:35	Kiruna 67.9° N, 21.1° E	high lat. spring 78.9–94.7°	LPMA/DOAS mini-DOAS	Nadir fixed Limb during ascent scanning Limb at float	5545: 11:07, 11:10 5558: 9:01
9 Oct. 2003 15:39–17:09	Aire-sur-l'Adour 43.7° N, 0.25° W	mid-lat fall 66–88°	LPMA/DOAS mini-DOAS	Nadir fixed Limb	8407: 11:30 8421: 9:17
24 March 2004 13:55–17:35	Kiruna 67.9° N, 21.1° E	high lat. spring 72–98°	LPMA/DOAS mini-DOAS	fixed Limb during ascent scanning Limb at float	10798 10:35

(i) for the closest match orbits (Dorf et al., in preparation, 2004[1])

[1]Dorf, M., Bovensmann, H., Burrows, J. P., Butz, A., Bösch, H., Camy-Peyret, C., Chipperfield, M., Grunow, K., Goutail, F., Hendrick, F., Hrechanyy, S., Naujokat, B., Pommereau, J.-P., Van Roozendael, M., Rozanov, A., Sioris, C., Stroh, F., Weidner, F., and Pfeilsticker, K.: Balloon-borne stratospheric BrO measurements: Intercomparison with ENVISAT/SCIAMACHY BrO limb profiles, Atmos. Chem. Phys. Discuss., in preparation, 2004.

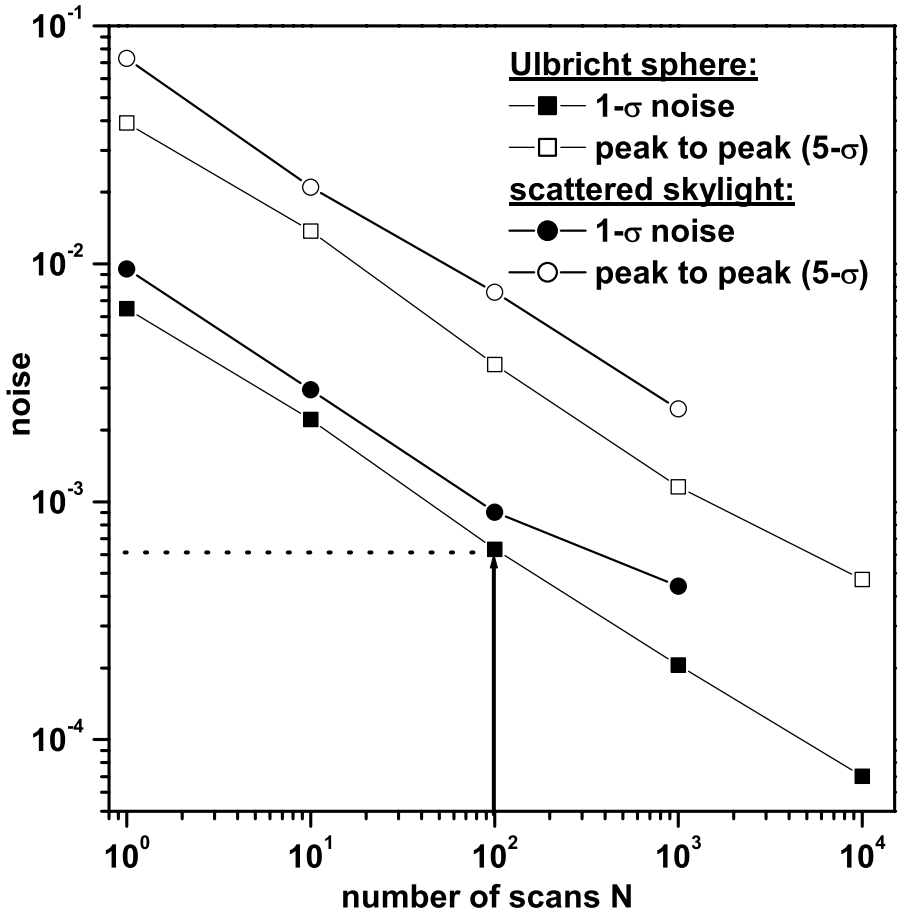

Fig. 1. Root mean square (1-σ) and peak to peak-to-peak residual structure (5-σ) as a function of co-added spectra N at 80% illumination level of the CCD array detector for white light of an Ulbricht sphere and skylight. The error indicates the (1-σ) noise actually achieved during the balloon flights.

ACPD
4, 7631–7665, 2004

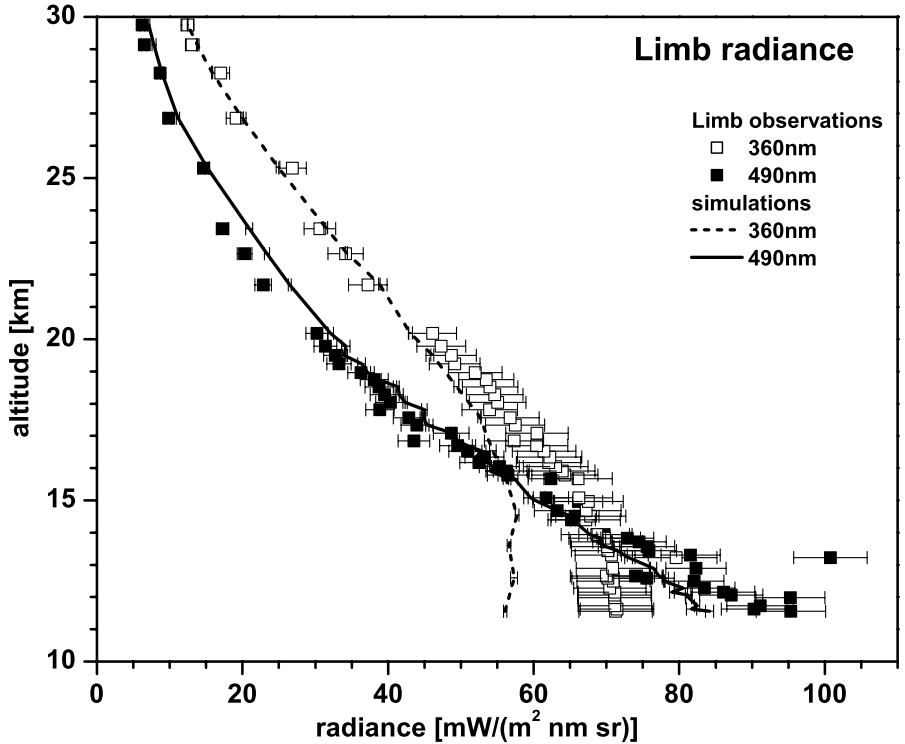

Fig. 2. Comparison of measured and simulated Limb radiance at 360 nm (open squares and dashed line) and 490 nm (filled squares and full line, respectively) for an azimuth angle of 90° and an elevation angle of +0.5° during balloon ascent over Kiruna on 23 March 2003.

ACPD
4, 7631–7665, 2004

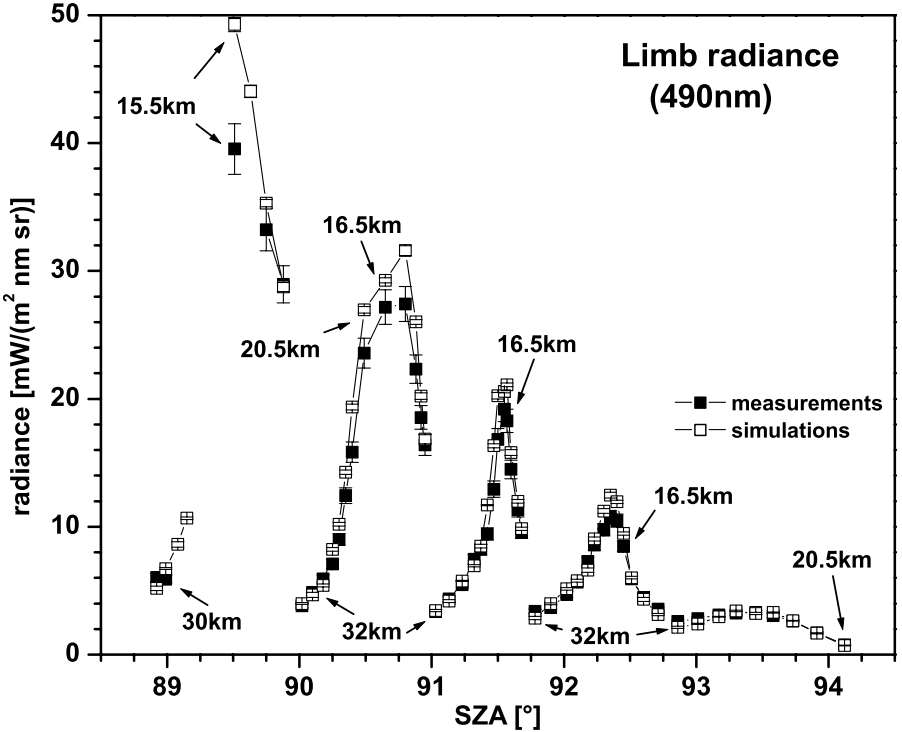

Fig. 3. Comparison of measured (filled squares) and forward modelled (open squares) Limb radiances at 490 nm for the Kiruna 23 March 2003, balloon flight at balloon float altitude (30.3–32.2 km). The figure shows 5 Limb profiling scans consisting of up to 13 individual observations each. The height labels denote the tangent heights of the observation.

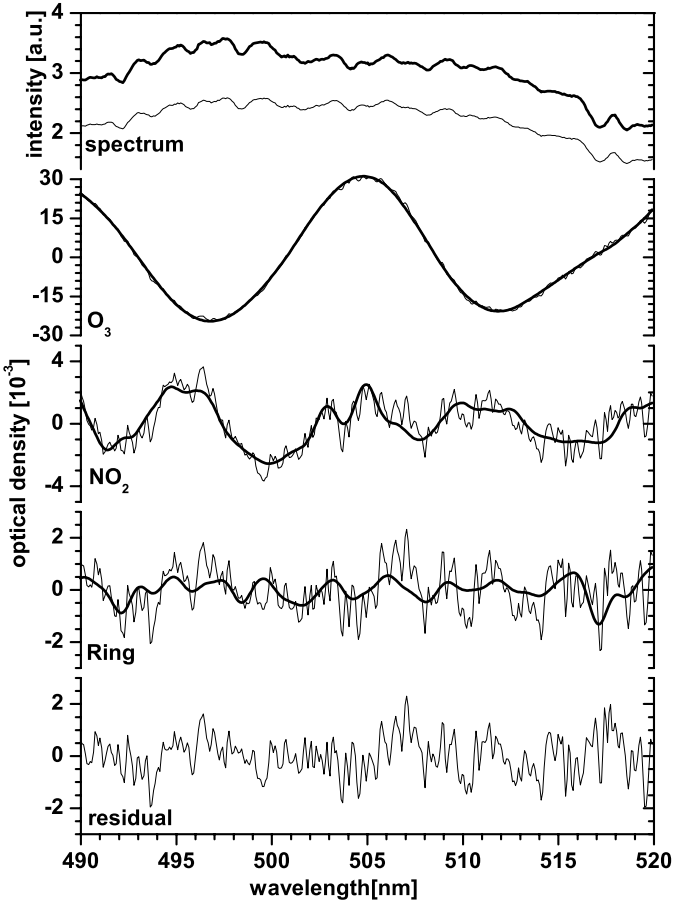

Fig. 4. Sample DOAS evaluation of ozone in the wavelength interval 490–520 nm for a Limb observation at float altitude in Limb scanning mode (at 31 620 km altitude, an elevation angle of −5.5°, azimuth angle of 90°, and SZA=89.9°) for the Kiruna flight on 23 March 2003. Shown is the retrieved slant column amount of O_3, NO_2, Ring (thick lines) and the latter plus the residual structure (thin lines). The upper two traces show the measured (thick line) and the Fraunhofer (thin line) spectra, the latter is recorded at an altitude of 29 746 km, an elevation angle of 0.5°, an azimuth angle of 90°, and SZA=88.5°.

ACPD
4, 7631–7665, 2004

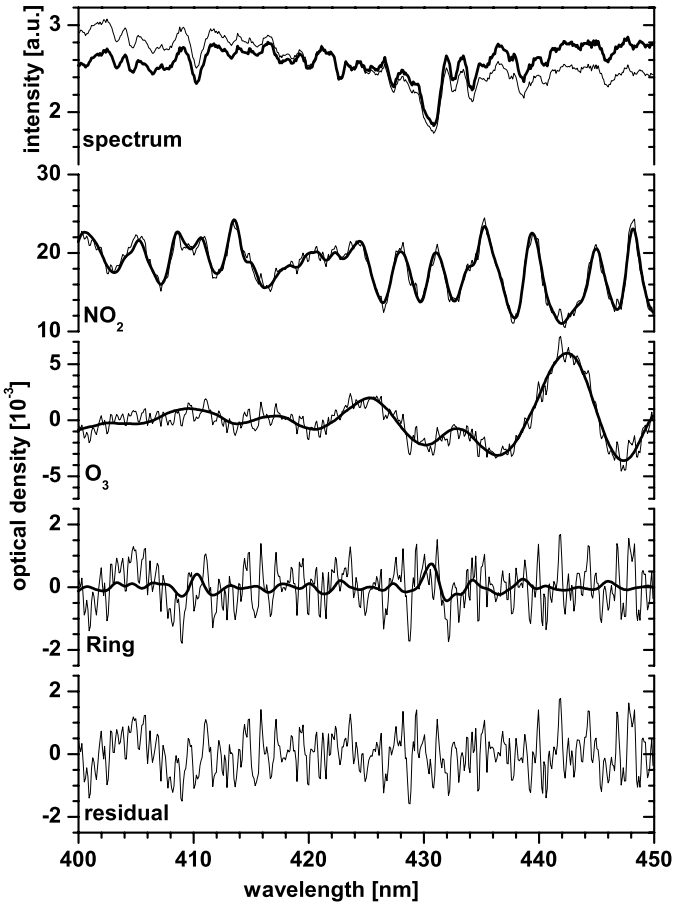

Fig. 5. same as Fig. 4 but for the NO_2 evaluation in the 400–450 nm wavelength interval and a Limb observation (at 30 940 km altitude, −3.5° elevation angle, 90° azimuth angle and SZA=89.4°) for the Kiruna flight on 23 March 2003.

ACPD
4, 7631–7665, 2004

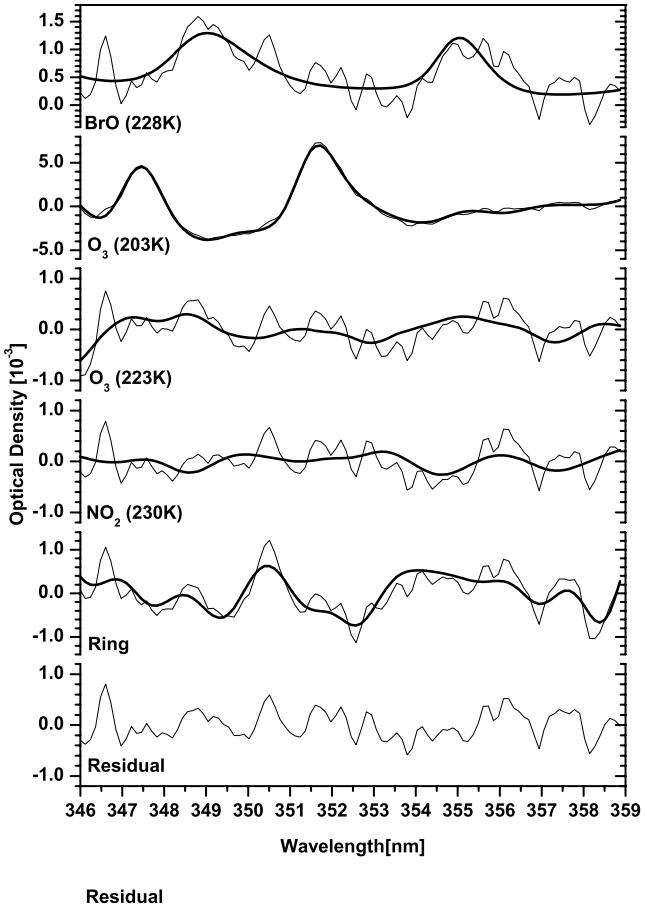

Fig. 6. same as Fig. 4 but for the BrO evaluation in the 347–358 nm wavelength interval and a Limb observation (at 26 439 km altitude, −1.5° elevation angle, 90° azimuth angle and SZA=82.9°) for the Kiruna flight on 24 March 2004.

ACPD
4, 7631–7665, 2004

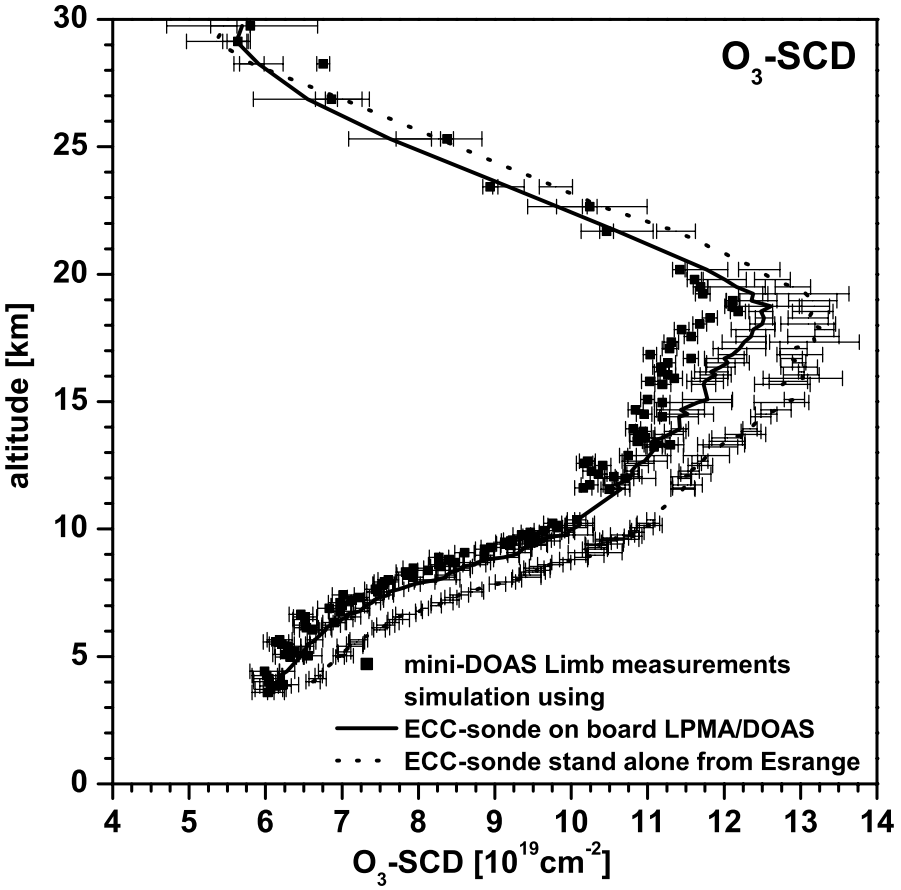

Fig. 7. Comparison of Limb (90° azimuth angle and 0.5° elevation angle) measured (filled squares)and forward modelled O_3-SCDs using the ozone measurements from two ECC-sondes deployed on the same gondola (full line), and flown stand-alone ~3 h after the LPMA/DOAS launch (dotted line) for the Kiruna 23 March 2003 flight.

ACPD
4, 7631–7665, 2004

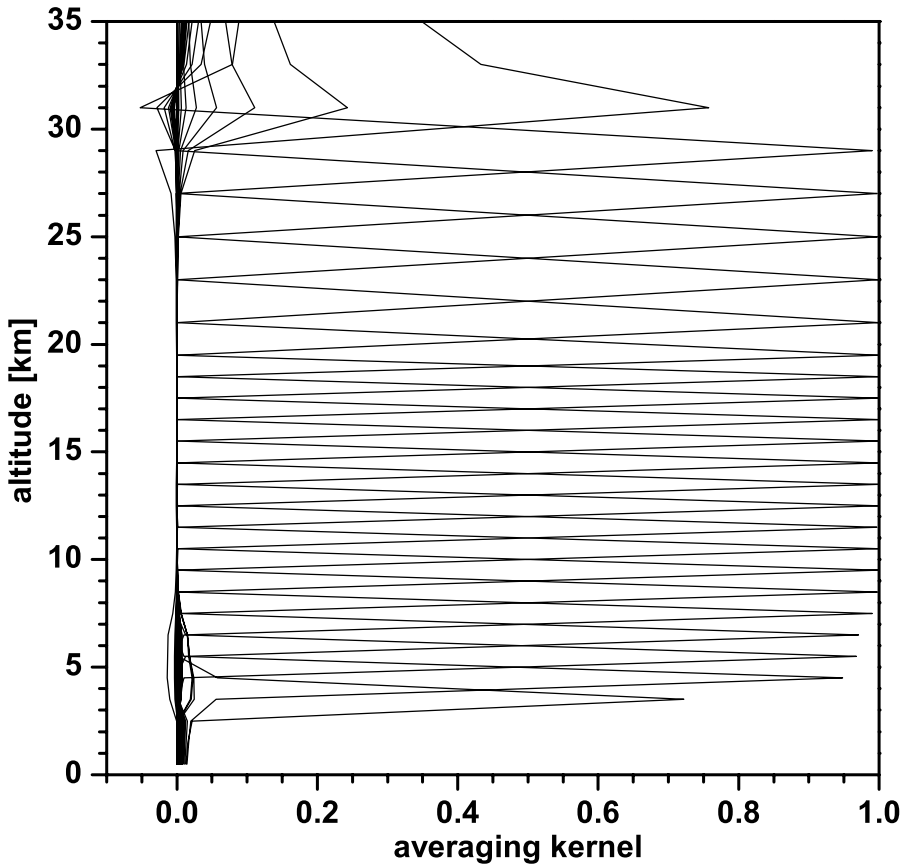

Fig. 8. Averaging kernel matrix for the ozone profile retrieval shown in Fig. 9.

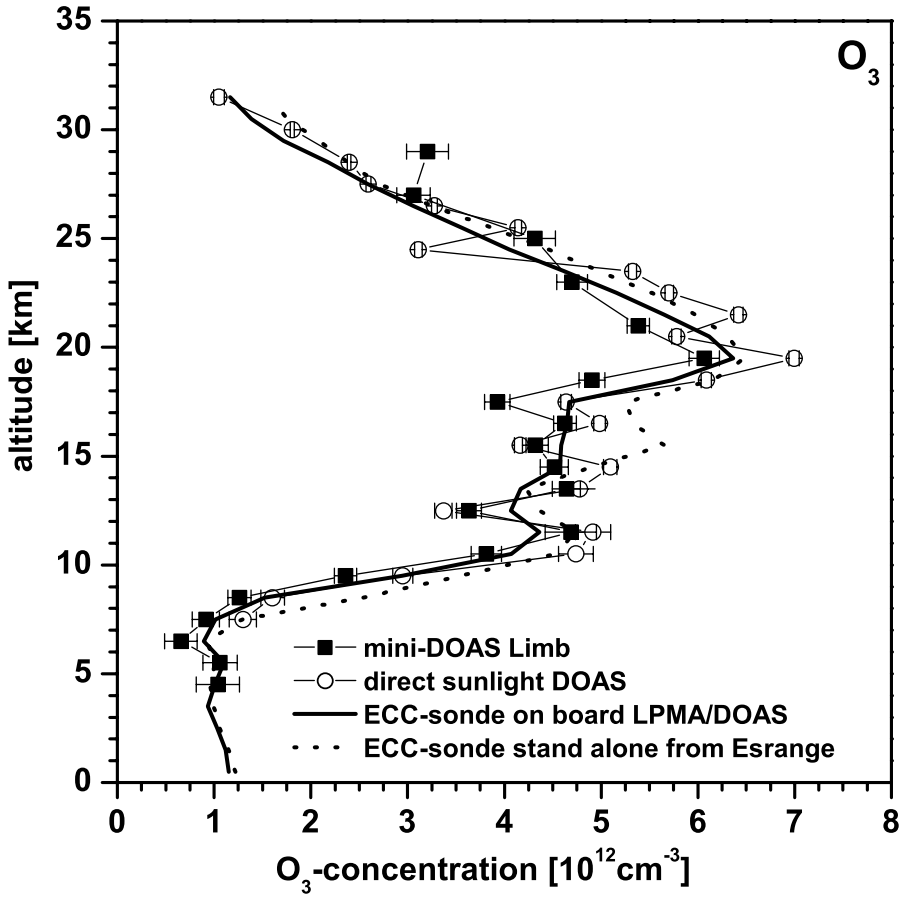

Fig. 9. Comparison of inferred O_3 profiles from (a) Limb observations (filled squares) at an azimuth angle of 90° and elevation angle of 0.5°, (b) the direct sunlight DOAS measurements (open circles), and two ECC ozone sondes (c) one deployed on the same gondola (full line) and (d) from the stand-alone launched ECC-sonde for the Kiruna, 23 March 2003 flight.

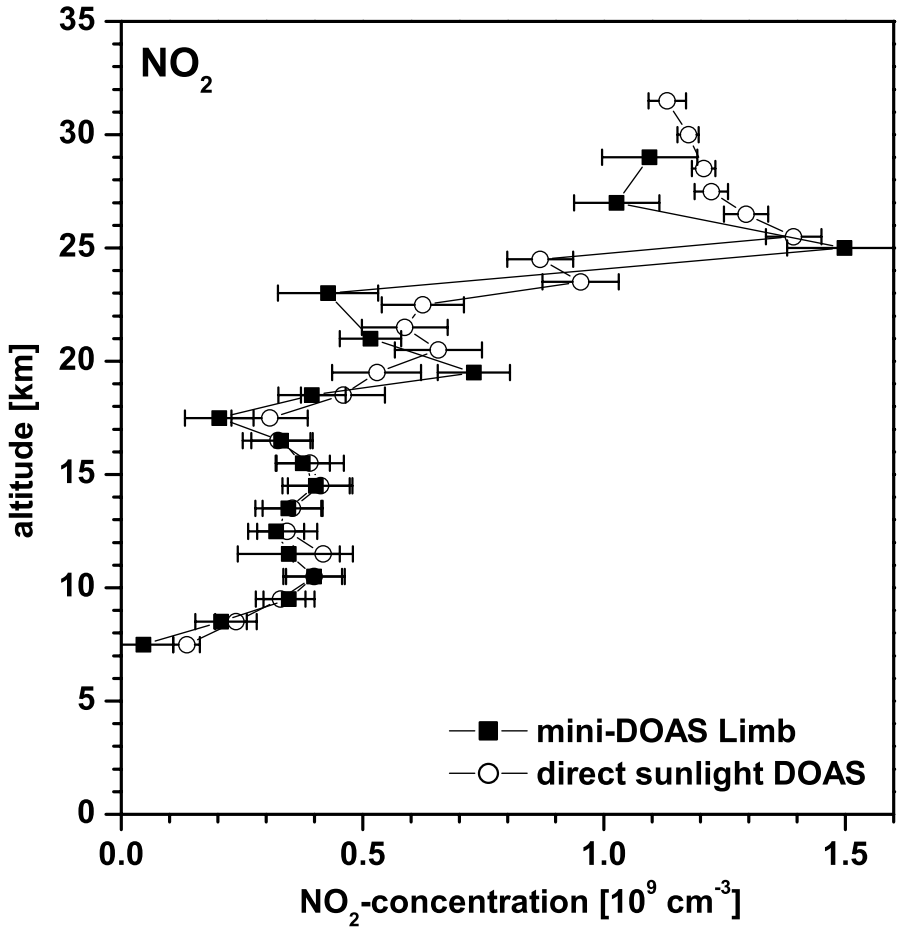

Fig. 10. Comparison of inferred NO_2 profiles from (a) Limb observations (filled squares) for an azimuth angle of 90° and elevation angle of 0.5°, and (b) from direct sunlight DOAS measurements (open circles) during balloon ascent at Kiruna on 23 March 2003.

ACPD
4, 7631–7665, 2004

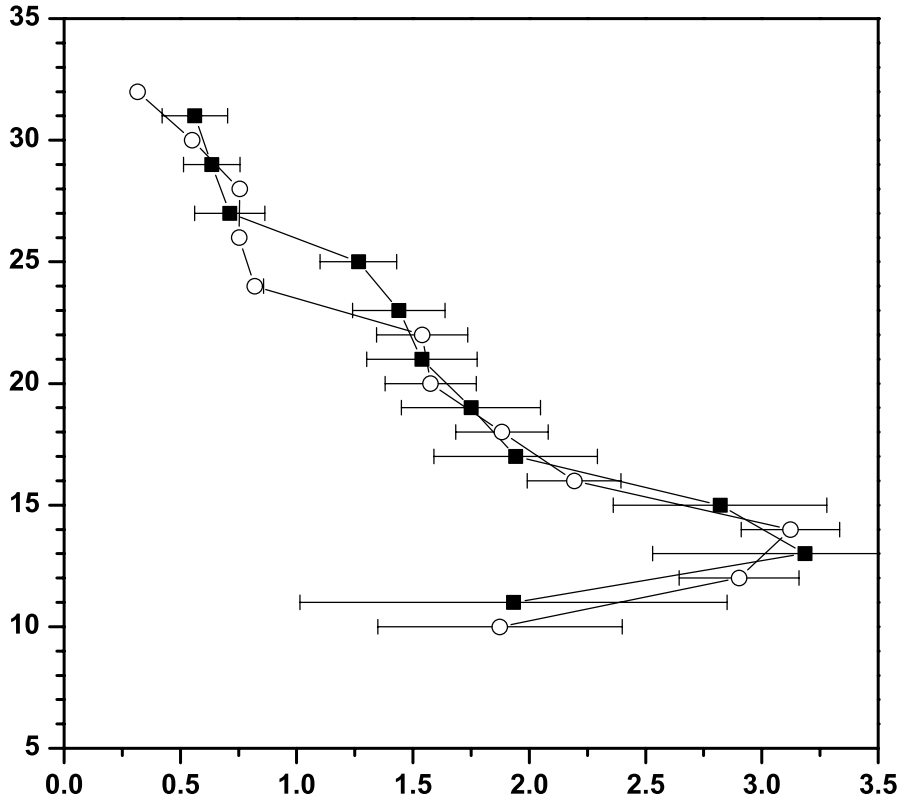

Fig. 11. Comparison of inferred BrO profiles from (a) Limb observations (filled squares) for an azimuth angle of 90° and elevation angle of −1.5°, and (b) from direct sunlight DOAS measurements (open circles) during balloon ascent at Kiruna on 24 March 2004.

ACPD
4, 7631–7665, 2004

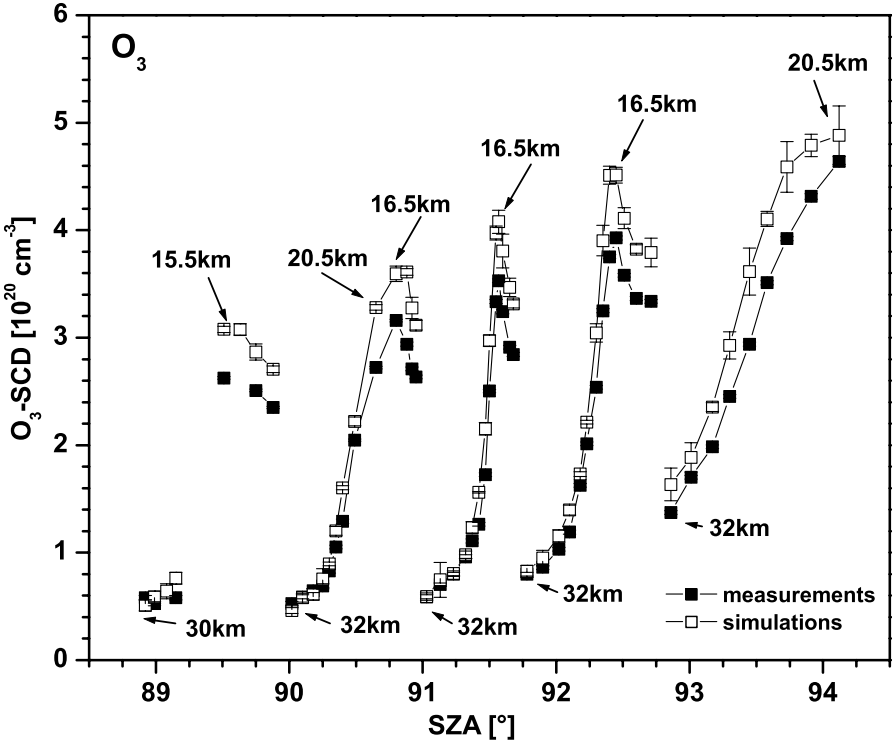

Fig. 12. Comparison of measured (filled squares) and forward modelled (open squares) Limb absorption of ozone for the Kiruna flight on 23 March 2003. The height labels denote the tangent heights of the observation.

ACPD
4, 7631–7665, 2004